

Original Article

LRP1 mitigates intervertebral disc degeneration by inhibiting endoplasmic reticulum stress through stabilizing the PPAR γ

Dengbo Yao^{a,b,1}, Ming Li^{a,1}, WeiKe Zeng^{c,1}, Kun Wang^d, Zhuangyao Liao^a, Enming Chen^a, Tong Xing^e, Yuwei Liang^a, Jun Tang^a, Guoming Wen^d, Qing Ning^a, Yuxi Li^{a,*}, Lin Huang^{a,**}

^a Department of Orthopedics Surgery, Sun Yat-sen Memorial Hospital, Sun Yat-sen University, Guangzhou, 510120, China

^b Department of Orthopedic Research Institute, West China Hospital, Sichuan University, Chengdu, Sichuan, China

^c Department of Radiology, Sun Yat-sen Memorial Hospital, Sun Yat-sen University, Guangzhou, 510120, China

^d Department of Orthopedics Surgery, The Eighth Affiliated Hospital, Sun Yat-sen University, Shenzhen, 518033, China

^e Department of Orthopedics, Shanghai Key Laboratory of Orthopedics Implant, The Ninth People's Hospital, Shanghai Jiao Tong University School of Medicine, Shanghai, 200011, China



ARTICLE INFO

Keywords:

Apoptosis
Endoplasmic reticulum stress
Extracellular matrix
Intervertebral disc degeneration
LRP1
Nucleus pulposus cells

ABSTRACT

Background: Intervertebral disc degeneration (IDD) is a significant cause of lower back pain, characterized by inflammation-mediated extracellular matrix (ECM) degradation, apoptosis, and aging of nucleus pulposus (NP) cells. Identifying key regulatory targets for these processes is crucial for IDD treatment. Previous research has highlighted the role of low-density lipoprotein receptor-related protein 1 (LRP1) in regulating ECM levels and cell fate, but its role in IDD remains under-explored. This study aims to elucidate the function and mechanism of LRP1 in the progression of IDD.

Methods: LRP1 expression was assessed in clinical tissue samples from patients diagnosed with IDD and in a rat IDD model established using needle puncture injuries. The effects of LRP1 knockdown and treatment with the LRP1 activator SP16 on apoptosis and ECM metabolism in NP cells were analyzed, with a focus on their relationship with endoplasmic reticulum (ER) stress. The interaction and regulatory mechanism between LRP1 and peroxisome proliferator-activated receptor gamma (PPAR γ) were further explored to clarify how LRP1 regulates ER stress. Finally, the in vivo therapeutic effect of SP16 was investigated using a rat tail IDD model.

Results: We found that LRP1 expression was significantly downregulated in IDD. In NP cells with LRP1 knockdown, there was a marked increase in apoptosis and detrimental ECM remodeling, which were associated with the activation of ER stress. Our research further revealed that LRP1 interacts with PPAR γ , stabilizing the PPAR γ protein and preventing its lysosomal degradation, thereby mitigating ER stress. Activation of LRP1 in our models significantly reduced ER stress, matrix degradation, and apoptosis, thereby attenuating IDD both in vitro and in vivo.

Conclusion: This study systematically investigated the role and mechanisms of the LRP1/PPAR γ /ER stress signaling axis in IDD. Our findings suggest that targeting LRP1 to modulate this signaling pathway could provide a promising therapeutic approach for the treatment of IDD.

The Translational potential of this Article: Our study demonstrated that LRP1 can reduce apoptosis and ECM degradation by inhibiting ER stress through stabilizing PPAR γ , indicating that targeting LRP1 may be a novel therapeutic strategy for IDD.

1. Introduction

Low back pain (LBP) is a multifaceted condition influenced by

biological, psychological, and social factors, significantly impacting quality of life and social function. Epidemiological data reveal a high prevalence of LBP, affecting approximately 70 %–85 % of individuals at

* Corresponding author.

** Corresponding author.

E-mail addresses: liy73@mail.sysu.edu.cn (Y. Li), huangl5@mail.sysu.edu.cn (L. Huang).

¹ These authors contributed equally to this work.

some point in their lifetime [1], which not only negatively impacts overall health but also imposes a substantial socioeconomic burden [2, 3]. Intervertebral disc degeneration (IDD) is the major cause of LBP, accounting for 40 % of all cases [4]. Advanced age is the greatest risk factor for IDD, and it is associated with processes such as excessive remodeling of the nucleus pulposus (NP) tissue, metabolic disorders of extracellular matrix (ECM) metabolism, excessive cell apoptosis, cellular senescence, and inflammation in NP cells [5–7].

Low-density lipoprotein receptor-related protein 1 (LRP1) a widely expressed transmembrane protein, is involved in diverse cellular processes such as lipid metabolism, endocytosis, signal transduction and has an anti-inflammatory effect [8–11]. In osteoarthritis (OA), LRP1 protein was decreased [12], which inhibit the interaction between LRP1 and extracellular harmful molecules such as aggrecanases [13], collagenases and tissue inhibitor of metalloproteinases [14], causes the metabolic homeostasis of the cartilage matrix to shift to a state of degradation and cell death [15,16]. Beyond its endocytic function, LRP1 also possesses extensive signal transduction capabilities, such as regulating pathways like PI3K/AKT [17], MAPK [18], NF-κB [19], WNT [20], and NOTCH [21], thereby influencing cellular processes such as survival, differentiation, proliferation, oxidative stress, apoptosis, inflammation, and autophagy. Previous studies have shown that LRP1 mitigates inflammation and oxidative stress, and plays a role in inhibiting apoptosis in ECM metabolism [16,22,23]. In our experiment, we found for the first time that in human degenerative NP tissue, rat IDD model, and in vitro IDD model, the expression of LRP1 is downregulated, and LRP1 knockout also indicate an increase in NP cell apoptosis and ECM decomposition.

Endoplasmic Reticulum Stress (ER stress) is a physiological or pathological process that occurs within cells, associated with adverse environmental factors such as inflammation and reactive oxygen species (ROS), leading to apoptosis and impairing the balance of ECM metabolism in IDD [24–26]. Additionally, LRP1 has been reported to negatively regulate ER stress in palmitate-induced steatosis in Hepatocytes [27]. In our preliminary experiments, we observed that a reduction in LRP1 activates ER stress. Therefore, we speculate that LRP1’s role in IDD may be mediated through the regulation of ER stress levels.

Peroxisome proliferator-activated receptor gamma (PPARγ) is a member of the ligand-activated nuclear transcription factor family that also plays an important role in regulating lipid metabolism, inflammatory responses, and cell differentiation [28]. Recent research indicates that PPARγ agonists, such as pioglitazone, effectively counteract inflammation and degeneration in intervertebral discs by suppressing the NF-κB signaling pathway [29]. Additionally, a miR-96-5p inhibitor in the context of IDD has indicated that regulating the PPARγ/NF-κB pathway can alleviate IDD [30]. This further reinforces the understanding of PPARγ’s role in managing the inflammatory and degenerative processes in IDD. Furthermore, studies have demonstrated the regulatory effect of LRP1 on PPARγ, such as their interaction playing a protective role in cardiovascular health [31]. In our study, we found that LRP1 interacts with PPARγ. In addition, PPARγ was also confirmed to inhibit ER stress [32]. Therefore, we hypothesize the function of LRP1 may be mediated through the regulation of ER stress by PPARγ.

Therefore, in this study, we will investigate the specific role and molecular mechanisms of LRP1 and its activator SP16 in regulating ECM metabolism and apoptosis of NP cells and validate these findings at the animal level, providing evidence for the potential of LRP1 as a therapeutic target for the treatment of IDD.

2. Materials

2.1. Patient samples

Human NP tissue for this experiment was collected from 12 patients (9 males and 3 females; aged 19–61; mean age = 39.33 ± 12.81 years) diagnosed with intervertebral disc degeneration (IDD) due to spinal

Table 1
Information on human disc samples from 12 patients.

Human disc samples	Sex	Age	Level	BMI	Grade
1	M	56 y	T11/12	22.9	I
2	M	25 y	L4/5	26.6	I
3	M	33 y	C5/6	25.1	II
4	F	32 y	L5/S1	22.7	II
5	M	19 y	L4/5	21.3	II
6	F	29 y	L4/5	22.1	III
7	M	33 y	C4/5	23	III
8	M	37 y	L4/5	25.95	III
9	M	47 y	L4/5	27.8	IV
10	M	44 y	L4/5	21.76	IV
11	F	56 y	L4/5	23.53	IV
12	M	61 y	L4/5	29	IV

F female, M male, y year.

deformity, lumbar spinal stenosis, spondylolisthesis, lumbar disc herniation, or spinal tumors, who underwent spine surgery at Sun Yat-sen Memorial Hospital of Sun Yat-sen University. MRI examinations were routinely performed before the operation, and the Pfirrmann grade was evaluated by three observers according to a previous report [33], was evaluated by three observers. Detailed information about the participants can be found in Table 1. The protocol for immunohistochemical staining of patient tissues was approved by the Ethics Committee of Sun Yat-sen Memorial Hospital of Sun Yat-sen University (NO. SYSEC-KY-KS-2021-356).

2.2. Rat IDD model and in vivo experiment

A total of 25 male rats, aged 8 weeks, were used in the experiment. For the construction of the IDD model, there were two groups with 5 rats each: the sham group and the annulus fibrosus puncture (AFP) group. For the in vivo experiments, rats were randomly divided into three groups: the sham group, the AFP group, and the SP16 group, with 5 rats in each group. The rat model of IDD was induced using the AFP technique. Briefly, the male SD rats were intraperitoneally anesthetized with pentobarbital sodium (5 mg/100 g body weight). After disinfecting the tail with 75 % alcohol, a 21G puncture needle was vertically inserted into the intervertebral disc, rotated 360°, and held in place for 30 s. The sham group underwent only skin puncture without entering the intervertebral disc. For the SP16 group, SP16 (10 μM; 4 μl) was immediately injected locally after the puncture, with subsequent reinjections on the 7th, 14th, and 21st days. To minimize the risk of additional damage from the injection process, all injections were administered using a 33-gauge Hamilton syringe (Hamilton Co., Reno, NV, USA). To control for volume effects, 4 μl of PBS was injected into the intervertebral disc of rats in the AFP group at the same time points. All animal experiments were conducted under the supervision of the Institutional Animal Care and Use Committee at Sun Yat-sen University and were approved by the Institutional Research Ethical Committee of Sun Yat-sen University (SYSU-IACUC-2024-000290).

2.2. Rat NP cell isolation

After euthanizing male SD rats, NP tissue was excised from the caudal intervertebral discs. The tissues were rinsed, minced, and digested at 37 °C with 0.25 % trypsin for 30 min, followed by a 3-h digestion with 0.2 % collagenase II at 37 °C. The rat cells were then cultured in Dulbecco’s Modified Eagle’s Medium (DMEM) containing 10 % fetal bovine serum (Gibco, USA) and 1 % penicillin-streptomycin (HyClone, Sv30010, USA) at 37 °C in a 5 % CO2 atmosphere.

2.3. In vitro siRNA and plasmid transfection

The rat NP cells were planted in a 6-well plate and transfected when the confluent of the cells reached 60–70 %. Small interference RNA

targeting rat LRP1 (sense: 5'-GCAAGUGGGUACCAACAAATT-3', anti-sense: UUUGUUGGUACCCACUUGCT).

T) and rat PPAR γ (sense: 5'-CCAUCGGAUUGAAGCUUAUTT-3', antisense: 5'-AUAAGCUUCAAUCGGAUGGTT-3') were synthesized by Gene Pharma (Shanghai, China). Transfection of siRNA was performed using Lipofectamine 3000 (Invitrogen) according to the description. RNA sequences targeting PPAR γ was cloned into the plasmids pCDH-CMV-MCS-EF1-CopGFP-T2A-Puro (Gene create, China) to overexpress PPAR γ . Lipofectamine 3000 and P3000 (Invitrogen) were used to plasmids transfection according to the description. The expression of related proteins was detected after transfection for 48 h.

2.3. Immunofluorescence

Rat NP cells were seeded in 24-well plates at a density of 3×10^4 cells per well. Following various treatments, the cells were fixed with 4 % paraformaldehyde for 30 min and then permeabilized with 0.5 % Triton X-100 for 5 min. The cells were washed with PBS and blocked with 10 % goat serum for 1 h at room temperature. Subsequently, the cells were incubated overnight with the relevant antibodies at 4 °C. For visualization, the cells were exposed to Alexa Fluor 488/594-tagged goat anti-rabbit/mouse IgG secondary antibody (1:200 dilution) and DAPI solution (10 μ g/mL) for 60 min at room temperature. Visualization was performed using an inverted fluorescence microscope (Olympus, IX73, Japan).

2.4. Histological and immunohistochemical analysis

Patient intervertebral disc tissue and rat in vivo intervertebral disc tissues were fixed with 4 % paraformaldehyde for 3 days. The rat intervertebral disc tissues were then decalcified in 20 % EDTA solution at room temperature for 1 month, with the EDTA solution being refreshed every 3 days, before being embedded in paraffin for sectioning. After deparaffinization using xylene and gradient ethanol, hematoxylin-eosin (HE) staining (Solarbio, G1120) and safranin O and fast green staining (Solarbio, G1371) were performed according to the product instructions. For immunohistochemical staining, antigen retrieval was performed using sodium citrate at 100 °C in a microwave oven for 10 min. After blocking with 10 % goat serum, the slides were incubated with relevant antibodies overnight at 4 °C. The slides were then treated with DAB solution (ZSGB-BIO, ZLI-9017, China) followed by a 30-s counterstain with hematoxylin. The results were visualized and captured using a microscope (Nikon, NI-U, Japan). The immunohistochemical images were analyzed using ImageJ to measure the average optical density (AOD) of positive areas, where AOD is calculated as IntDen/Area. The histological grading of IDD was based on previous research [34].

2.5. Transmission electron microscope (TEM) scanning

The rat NP cells were planted in 6-well plates. After relevant treatments, the cells were digested, and collected. Discard the supernatant, gently added 1 ml of electron microscope stationary solution and fix it at room temperature for 1 h, then transfer it to a refrigerator at 4 °C overnight. The cell specimens were sent to Guangzhou tenng Biotechnology Co., Ltd for sample preparation and electron microscope scanning (FEI, Tecnai G2 Spirit).

2.6. Western blot

RIPA lysis buffer containing 1 % protease inhibitor and 1 % phosphatase inhibitor was used to extract total protein from NP cells. The protein concentration was determined using a BCA kit (CwBio, CW0014, China). Protein samples (30 μ g/lane) were separated via FuturePAGE™ prefabricated gel with a concentration of 4–12 % (ACE) and electrotransferred onto polyvinylidene difluoride (PVDF) membranes

(Millipore, USA). After blocking with 5 % skimmed milk at room temperature for 1 h, the membranes were incubated overnight at 4 °C with the following primary antibodies: anti-LRP1 (1:20000, Abcam, ab92544), anti-COL2 (1:1000, Abcam, ab34712), anti-MMP13 (1:1000, Abcam, ab39012), anti-BCL2 (1:1000, Immunoway, YT0470), anti-cleaved Caspase3 (1:1000, CST, 9661), anti-GRP78 (1:2000, Immunoway, YT5858), anti-CHOP (1:1000, Immunoway, YM3668), anti-p-PERK (1:500, Immunoway, YP1055), anti-PERK (1:1000, Immunoway, YT3666), anti-p-eIF2 α (1:1000, Immunoway, YP0093), anti-eIF2 α (1:1000, Immunoway, YT1507), anti-ATF4 (1:1000, Immunoway, YT1102), anti-PPAR γ (1:1000, Immunoway, YT3836), anti-GAPDH (1:2000, CwBio, CW0100M), and anti- β -Tubulin (1:2000, CwBio, CW0098M). Following three PBS washes, the membranes were exposed to the secondary antibody for 1 h at room temperature. Protein bands were visualized using enhanced chemiluminescence with the imaging systems (BLT, GelView 6000 pro, China and GBOXChemi-XT4, Germany).

2.7. Flow cytometry

The apoptosis of rat NP cells were measured by flow cytometry. The cells were stained with annexin V/FITC and propidium iodide (PI) at room temperature in the dark for 15 min using Annexin V Apoptosis Detection Kits (Invitrogen, BMS500FI, USA). Then, the apoptosis of NP cells was measured by Flow Cytometer (BD, FACSVerser, USA).

2.8. Co-immunoprecipitation (co-IP)

The rat NP cells were implanted in 10 cm dish and transfected with plasmid to overexpress PPAR γ . The cells lysate was collected on ice and incubated with 4 μ g primary antibody at 4 °C overnight: anti-LRP1 (Abcam, ab92544), anti-PPAR γ (Proteintech, 16643-1-AP). Then, antigen-antibody complex was mixed with 30 μ L protein A/G magnetic beads (Thermo, 88804) at room temperature for 1 h. Washing the magnetic beads for 3 times, the eluted protein was obtained using elution buffer for 15 min. Considering that the molecular weight of PPAR γ is close to the heavy chain, we used mouse PPAR γ antibody (1:1000, SAB, 27024) for immunoblotting analysis.

2.9. Quantitative reverse transcription polymerase chain reaction (qRT-PCR)

Total RNA was isolated from rat NP cells using EZ-press RNA Purification Kit (EZBioscience, B004D, USA). Reverse transcription was performed using the Prime Script RT Master Mix kit (Takara). The process of qRT-PCR was performed using the SYBR Green Premix (Accurate Biology, AG11701, China) on LightCycler 96 System (Roche). Ct values were normalized to β -actin as an endogenous control, and relative expression were computed by using $2^{-\Delta\Delta Ct}$ method. The sequences of the primers are listed as follows: β -actin (sense: 5'-TCTCTGCTCCTCCCTGTTC-3', anti-sense: 5'-ACACCGACCTTCAC-CATCT-3'); LRP1 (sense: 5'-ATGTGGCTGTGTTG.

AAGGATAC-3', antisense: 5'-GCTCGTAGGTGTGATGGTAGA-3'); PPAR γ (sense: 5'-TCGCAAGGTGCTCCAGAAGAT3', anti-sense: 5'-GAAGGCTCATATCTGTC TCCGTCTT-3').

2.10. Magnetic resonance imaging (MRI) analysis

After completing the relevant treatments, the rats were euthanized using an overdose of sodium pentobarbital (150 mg/kg). The rat tails were then removed and promptly subjected to MRI scans using a Siemens Magnetom Vida 3.0T (Siemens Healthineers, Erlangen, Germany). The scan settings were: TR 2700 ms, TE 70 ms, resolution 0.29×0.29 mm, slice thickness 2 mm, and FOV 150×112.5 mm. Based on the MRI images, the extent of IDD was quantified using the Pfirrmann grading criteria for spinal discs.

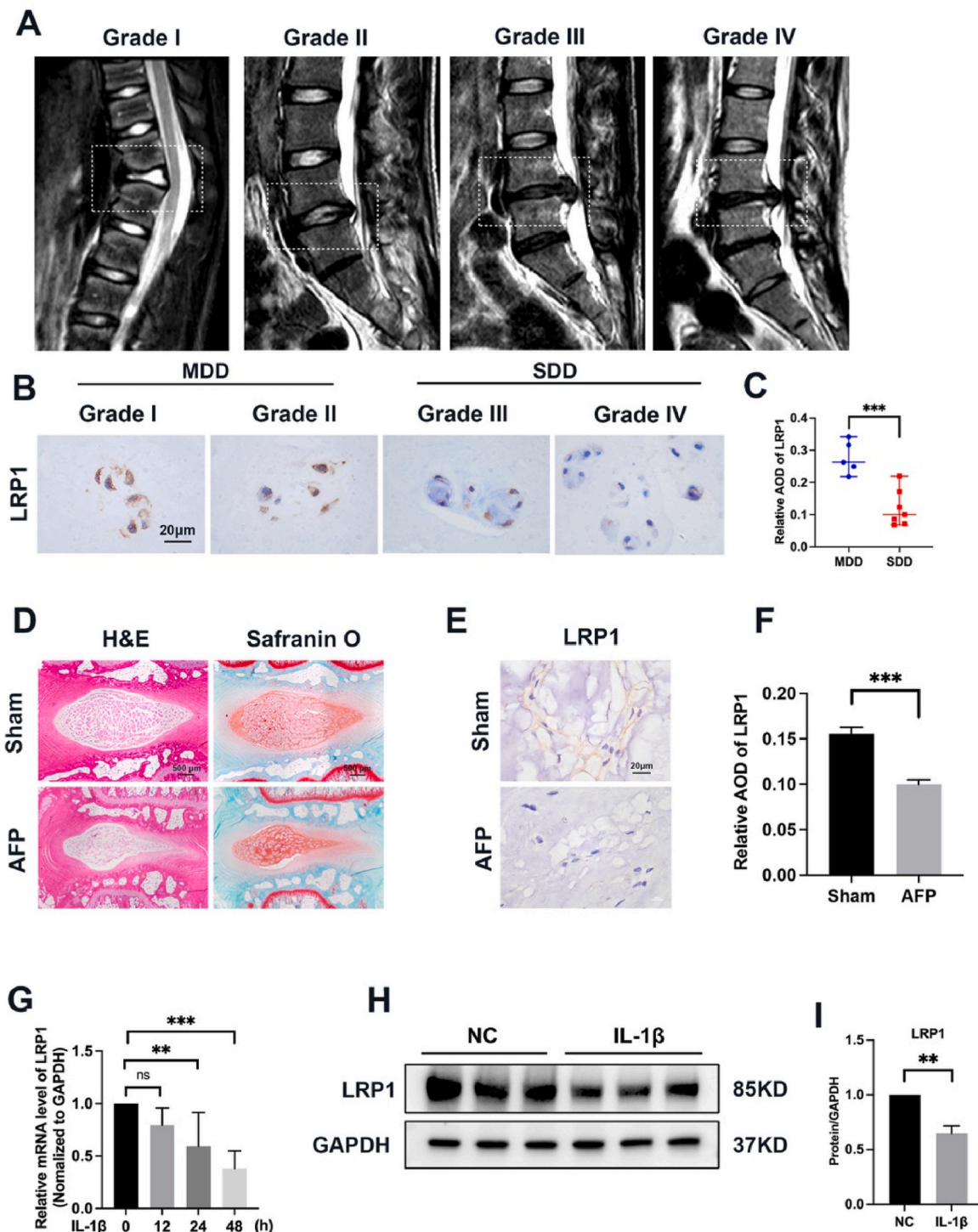


Fig. 1. LRP1 was downregulated in the human degenerative NP tissue and rat model established by annulus fibrosus puncture. **A** MRI images of human intervertebral discs with different Pfirrmann grades: mild disc degeneration (n = 5) and severe disc degeneration (n = 7). **B, C** Expression of LRP1 was decreased in human NP tissue with severe disc degeneration compared to mild disc degeneration, as detected by immunohistochemical staining. **D** HE and safranin O staining of rat intervertebral disc treated by sham operation and annulus fibrosus puncture for 4 weeks (n = 3). **E, F** Expression of LRP1 was downregulated in annulus fibrosus puncture group (n = 3) compared to sham group (n = 3), as assayed by immunohistochemical staining. **G** The relative mRNA expression of LRP1 in rat NP cells was measured by qRT-PCR (n = 3). **H, I** Western blot analysis of LRP1 in rat NP cells treated with IL-1 β (20 ng/ml) for 48 h (n = 3). *p < 0.05, **p < 0.01, ***p < 0.001. Data are presented as the mean \pm SD.

2.11. Statistical analysis

To examine data with normal distribution and equal variance, a standard one-way ANOVA, complemented by Tukey's test for multiple comparisons, was employed for groups of three or more. For

comparisons between two groups, a two-tailed Student's t-test without pairing was utilized. Values are presented as the mean \pm SD. Statistical significance was set as *P < 0.05, **P < 0.01, ***P < 0.001, with "ns" indicating no significance.

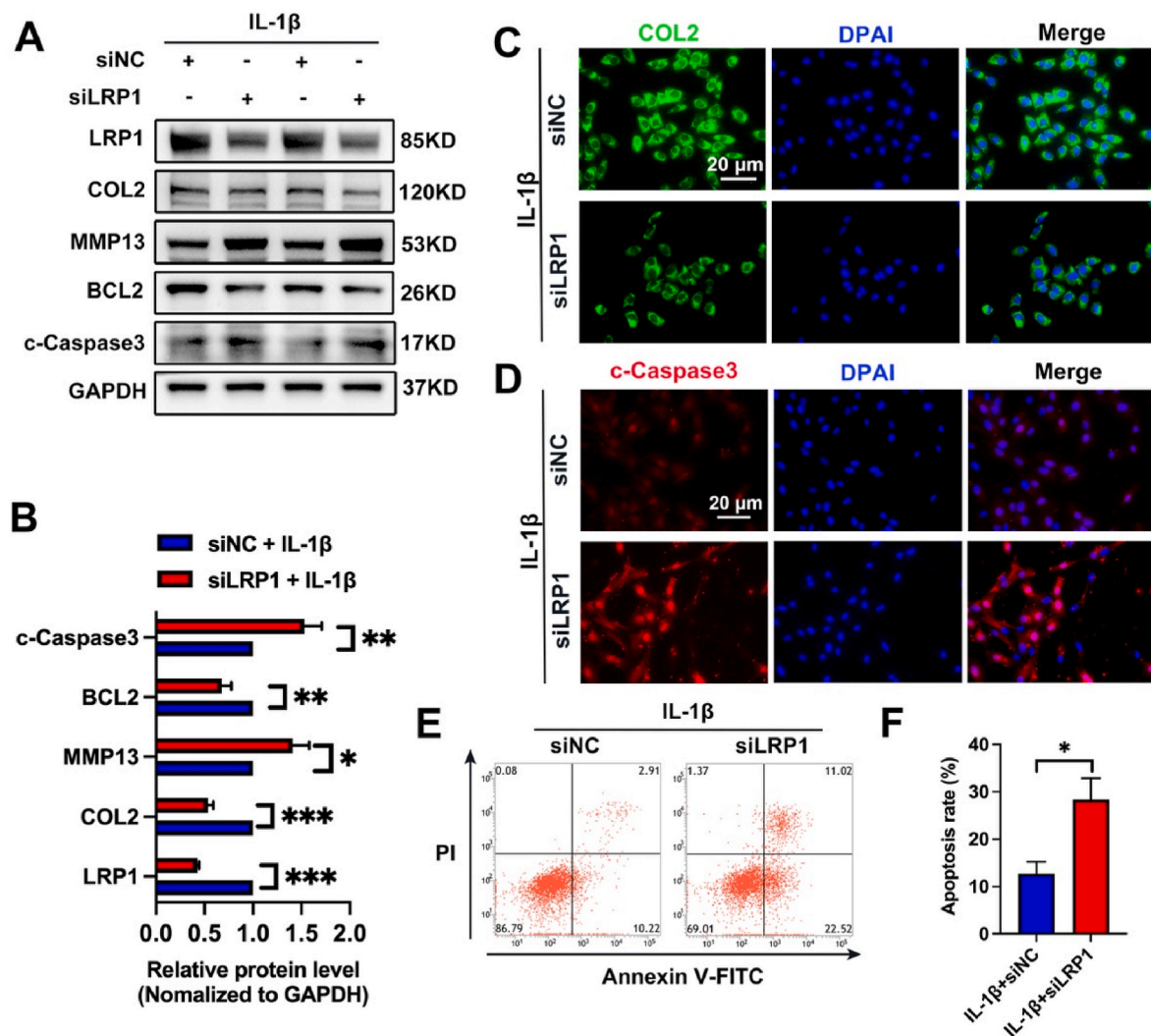


Fig. 2. Knockdown of LRP1 promoted apoptosis and ECM degradation in IL-1 β -treated NP cells. **A, B** Western blot analysis of anabolic marker (COL2), catabolic marker (MMP13), antiapoptotic marker (BCL2) and proapoptotic marker (cleaved caspase3) in siNC-treated and siLRP1-treated NP cells (n = 5). **C, D** Representative images of COL2 and cleaved caspase3 immunofluorescence in siNC-treated and siLRP1-treated groups (n = 3). **E, F** Apoptosis rate of rat NP cells by flow cytometry (n = 5). *p < 0.05, **p < 0.01, ***p < 0.001. Data are presented as the mean \pm SD.

3. Results

3.1. LRP1 was downregulated in the human degenerative NP tissue and rat model established by annulus fibrosus puncture

To clarify the role of LRP1 in IDD, we first collected grade I to grade IV intervertebral discs and defined grade I-II as mild disc degeneration (MDD) and III-IV as severe disc degeneration (SDD), according to the literature [6] (Fig. 1A). Immunohistochemical staining revealed that the SDD groups had lower expression of LRP1 than the MDD groups (Fig. 1B and C). HE and safranin O staining confirmed that the AFP-induced rat IDD model was successfully established (Fig. 1D). Immunohistochemical staining demonstrated that the expression of LRP1 was downregulated in the rat IDD model (Fig. 1E and F). Next, we stimulated rat NP cells with IL-1 β to construct an in vitro model of NP cell degeneration. Western blot analysis showed that IL-1 β stimulation downregulated the mRNA and protein levels of LRP1 (Fig. 1G–I), confirming a negative correlation between LRP1 and IDD.

3.2. Knockdown of LRP1 promoted apoptosis and ECM degradation in IL-1 β -treated NP cells

To clarify the role of LRP1 in IDD, we used siRNA to knock down LRP1 in rat NP cells. Western blot results showed that LRP1 was effectively knocked down by siRNA, leading to the downregulation of the protein level of COL2 and the upregulation of MMP13 (Fig. 2A and B). Furthermore, knockdown of LRP1 downregulated the protein level of BCL2 and upregulated the protein level of cleaved caspase-3 in IL-1 β -treated NP cells (Fig. 2A and B). Immunofluorescence also confirmed the western blot results of Col2 and cleaved caspase3 (Fig. 2C and D). Flow cytometry confirmed that knockdown of LRP1 significantly exacerbated IL-1 β -induced apoptosis (Fig. 2E and F). These results suggest that the reduction of LRP1 promotes ECM degradation and apoptosis of NP cells, indicating that LRP1 may play a role in inhibiting IDD.

3.3. Activation of LRP1 alleviated apoptosis and matrix degradation in IL-1 β -treated NP cells

Our previous experiments verified that knockdown of LRP1 promotes ECM catabolism, inhibits ECM synthesis, and leads to apoptosis of NP cells. Therefore, in the following studies, we investigated how the

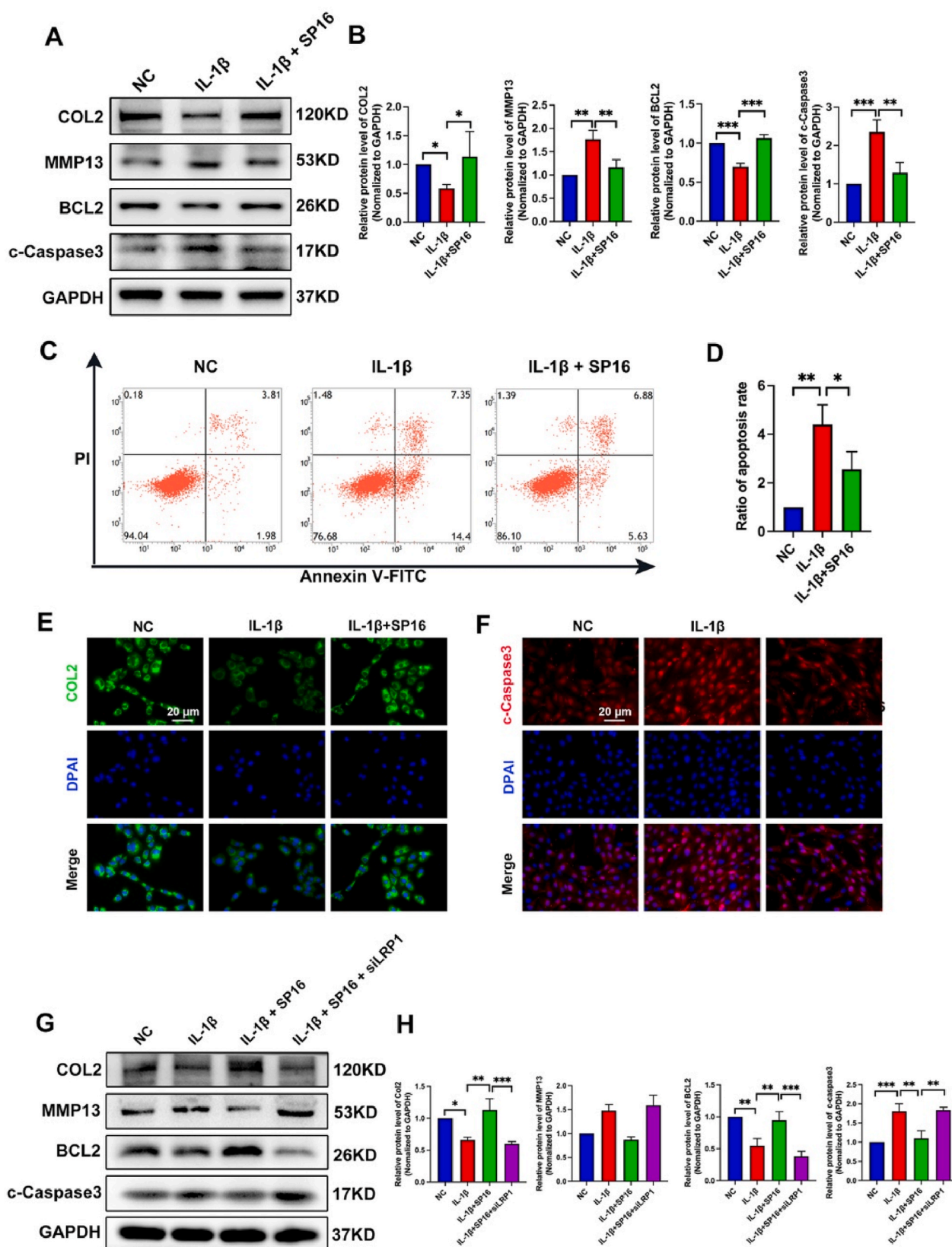
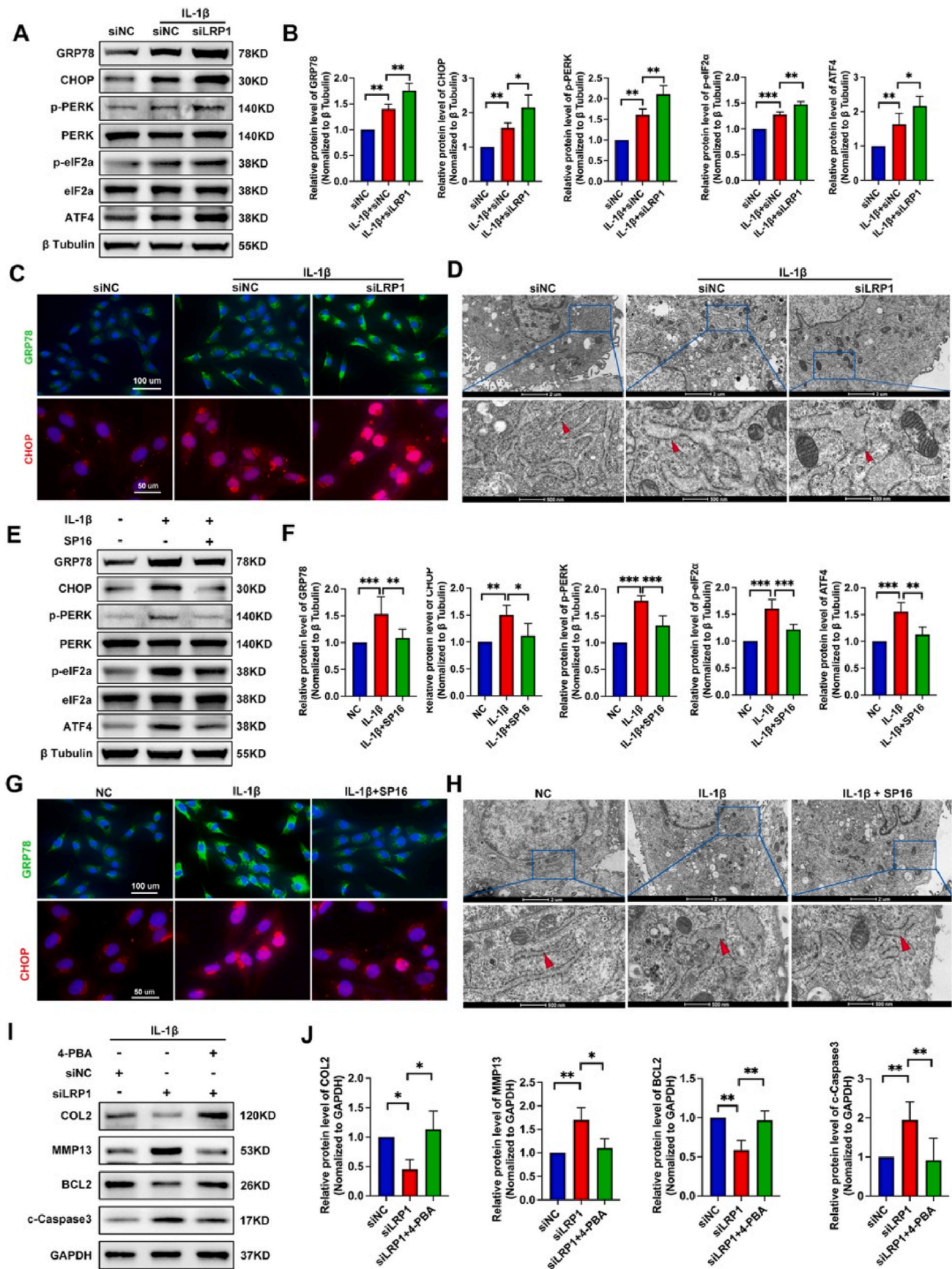


Fig. 3. Activation of LRP1 alleviated apoptosis and matrix degradation in IL-1 β -treated NP cells. **A, B** Western blot analysis of COL2, MMP13, BCL2 and cleaved caspase3 in NP cells of each indicated groups ($n = 3$). **C, D** Apoptosis rate of NP cells by flow cytometry ($n = 4$). **E, F** Representative immunofluorescence images of COL2 and cleaved caspase3 in NP cells of each indicated groups ($n = 3$). **G, H** Western blot analysis of COL2, MMP13, BCL2 and cleaved caspase3 in SP16-treated and siLRP1-treated rat NP cells ($n = 3$). * $p < 0.05$, ** $p < 0.01$, *** $p < 0.001$. Data are presented as the mean \pm SD.



(caption on next page)

Fig. 4. LRP1 inhibits ER stress induced by IL-1 β and ER stress-mediated matrix metabolism disorder and apoptosis in NP cells. A, B Western blot analysis of ER stress markers (GRP78, CHOP), ER stress signaling pathway (PERK, p-eIF2 α , ATF4) in NP cells treated with siNC and siLRP1 under IL-1 β stimulation (n = 3). C Representative immunofluorescence images showing GRP78 and CHOP in NP cells with knockdown of NC and knockdown of LRP1 under stimulation of IL-1 β (n = 3). D Representative TEM images showing the morphology of endoplasmic reticulum (n = 3). A low-field image of a whole cell and magnified high-field images are shown. Swollen endoplasmic reticulum is indicated by red arrows. E, F Western blot analysis of GRP78, CHOP, p-PERK, p-eIF2 α , ATF4 in NP cells treated with or without SP16 under IL-1 β stimulation (n = 4). G Representative immunofluorescence images of GRP and CHOP in NP cells of each indicated groups (n = 3). H Representative TEM images showing the morphology of endoplasmic reticulum. Swollen endoplasmic reticulum is indicated by red arrows. I, J Expression of COL2, MMP13, BCL2 and cleaved caspase3 in NP cells of each indicated groups (n = 4), as detected by western blot. *p < 0.05, **p < 0.01, ***p < 0.001. Data are presented as the mean \pm SD.

activation of LRP1 influences ECM metabolism, and the apoptosis of NP cells. SP16, agonist of LRP1, is a synthetic 17-amino acid peptide derived from the C-terminus of α 1-Antitrypsin (AAT), specifically designed based on the structural features and potential recognition sequences of LRP1 [35,36]. This peptide targets LRP1 and exerts anti-inflammatory effects [36,37]. The sequence of SP16 is Ac-VKFNKPFVFLNleIEQNTK-NH₂, where methionine (M) was substituted with norleucine (Nle) to enhance peptide stability and improve binding affinity to LRP1. SP16 was synthesized by All Peptide Biotechnology Co., Ltd. (Hangzhou, China) with a purity of 98 %. Western blot results indicated that the protein level of COL2 was upregulated and MMP13 was downregulated in SP16-treated NP cells under IL-1 β stimulation (Fig. 3A and B). Furthermore, the expression of cleaved caspase-3 decreased, and BCL2 increased simultaneously (Fig. 3A and B). In addition, immunofluorescence and flow cytometry further verified the western blot results (Fig. 3C–F). However, knockdown of LRP1 counteracted the effects of SP16, indicating that SP16 regulates apoptosis and ECM metabolism in nucleus pulposus cells in an LRP1-dependent manner (Fig. 3G and H).

3.4. LRP1 inhibits ER stress induced by IL-1 β and ER stress-mediated matrix metabolism disorder and apoptosis in NP cells

Endoplasmic reticulum (ER) stress has been confirmed to be associated with IDD. We speculated that the regulation of matrix metabolism and apoptosis in NP cells by LRP1 is related to ER stress. In our study, western blot results showed that the expression of GRP78, C/EBP homologous protein (CHOP), phosphorylated protein kinase-like endoplasmic reticulum kinase (p-PERK), phosphorylated eukaryotic initiation factor 2 alpha (p-eIF2 α), and activating transcription factor 4 (ATF4) increased under IL-1 β stimulation, and their expression was further upregulated by knockdown of LRP1 (Fig. 4A and B). Furthermore, GRP78, CHOP, p-PERK, p-eIF2 α , and ATF4 were significantly downregulated in SP16-treated NP cells compared to IL-1 β -treated NP cells (Fig. 4E and F). Immunofluorescence and TEM further verified the western blot results (Fig. 4C, D, G, H). Moreover, the matrix metabolism disorder and apoptosis caused by knockdown of LRP1 in IL-1 β -treated NP cells were rescued by the ER stress inhibitor 4-Phenylbutyric acid (4-PBA) (Fig. 4I and J). These results indicate that dysfunction of LRP1 leads to matrix metabolism disorder and apoptosis of NP cells, which is regulated, at least partly, by ER stress.

3.5. PPAR γ inhibits IDD and participates in LRP1-mediated inhibition of ER stress

PPAR γ has been confirmed to inhibit inflammation in the intervertebral disc, and it has been shown that PPAR γ can be regulated by LRP1 [31]. Therefore, we speculated that PPAR γ is a downstream target of LRP1 and is involved in the pathogenesis of IDD. Immunohistochemical results showed that PPAR γ expression in SDD groups was lower than in MDD groups, consistent with the expression of LRP1 (Fig. 5A and B). Western blot analysis demonstrated lower expression of PPAR γ in IL-1 β -treated NP cells, which is same as expression of LRP1 (Fig. 5C and D). To investigate the role of PPAR γ in IDD, we knocked down PPAR γ using siRNA and overexpressed PPAR γ via plasmid transfection. Western blot results showed that PPAR γ knockdown led to disrupted matrix

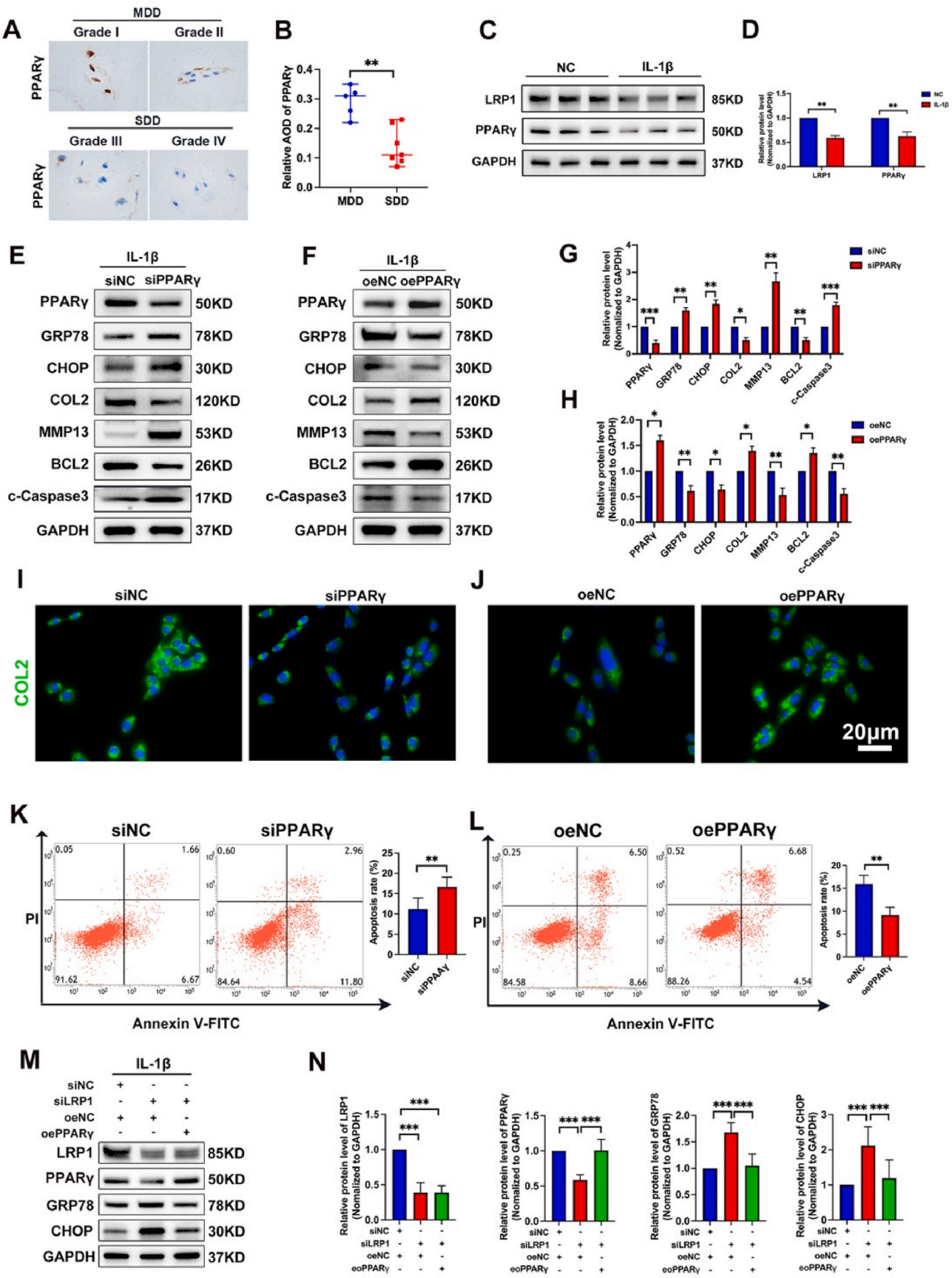
metabolism and an apoptotic phenotype in NP cells, as indicated by the downregulation of COL2 and upregulation of MMP13 (Fig. 5E, G). Additionally, there was a decrease in BCL2 expression and an increase in cleaved caspase-3 levels (Fig. 5E, G). In contrast, overexpression of PPAR γ produced the opposite effects, inhibiting ECM degradation and apoptosis (Fig. 5F, H). Moreover, knocking down PPAR γ increased ER stress levels, as evidenced by the upregulated expression of GRP78 and CHOP, while overexpression of PPAR γ reduced ER stress markers (Fig. 5E–H). Immunofluorescence and flow cytometry analyses further confirmed that PPAR γ negatively regulates ER stress and apoptosis, and inhibits matrix degradation (Fig. 5I–L), corroborating the western blot results. To determine whether PPAR γ is involved in LRP1-regulated ER stress, we knocked down LRP1 and overexpressed PPAR γ . Western blot results showed that GRP78 and CHOP expression increased following LRP1 knockdown but decreased upon PPAR γ overexpression, suggesting that ER stress is regulated by LRP1 through PPAR γ (Fig. 5M and N).

3.6. LRP1 interacted with PPAR γ to inhibit PPAR γ degradation via lysosomal pathway

To investigate the regulatory mechanism between LRP1 and PPAR γ , we knocked down LRP1 and examined PPAR γ expression. Western blot analysis showed that LRP1 knockdown reduced PPAR γ protein levels while slightly increasing its mRNA levels, suggesting that LRP1 is involved in the post-translational regulation of PPAR γ (Fig. 6A–C). We next examined the interaction between LRP1 and PPAR γ . Co-immunoprecipitation (co-IP) confirmed that LRP1 physically interacts with PPAR γ (Fig. 6D), and immunofluorescence analysis revealed that LRP1 and PPAR γ colocalize in the cytoplasm of NP cells, with overlapping fluorescence signals (Fig. 6E). To elucidate how LRP1 regulates PPAR γ protein levels, we used cycloheximide (CHX) to inhibit protein synthesis and observed that LRP1 knockdown accelerated PPAR γ protein degradation, while LRP1 activation inhibited PPAR γ degradation (Fig. 6F–I). Additionally, we explored the degradation pathway of PPAR γ using MG132 and chloroquine (Cq). Western blot results showed that MG132 had no effect on PPAR γ degradation in both siNC and siLRP1 groups. However, in Cq-treated NP cells, PPAR γ degradation was significantly inhibited in both siNC and siLRP1 groups (Fig. 6J–M). Furthermore, SP16 increased PPAR γ protein levels in CHX-treated and CHX-plus MG132-treated NP cells (Fig. 6N and O). These findings suggest that LRP1 stabilizes PPAR γ protein and inhibits its degradation via the lysosomal pathway.

3.7. SP16 attenuates IDD in rat model

To verify the effect of LRP1 on relieving IDD in vivo, SP16 was locally injected into the rat IDD model established by AFP (Fig. 7A). MRI analysis showed that the signal intensity of the intervertebral disc in the SP16 group was higher than that in the AFP group, and the Pfirrmann grading was also relatively lower (Fig. 7B and C). HE and Safranin O staining revealed that NP tissue was decreased or disappeared, and ECM was reduced in the AFP group. However, these changes were significantly alleviated in the SP16 group (Fig. 7D–F). Furthermore, immunohistochemical staining demonstrated that the expression levels of LRP1 and PPAR γ were reduced in the AFP group but elevated in the SP16 group (Fig. 7G, H, M, N). In contrast, GRP78, CHOP, and cleaved



(caption on next page)

Fig. 5. PPAR γ inhibits IDD and participates in LRP1-mediated inhibition of ER stress. **A, B** Expression of PPAR γ was decreased in human NP tissue with severe disc degeneration compared to mild disc degeneration, as detected by immunohistochemical staining. **C, D** Western blot analysis of LRP1 and PPAR γ in NP cells treated with IL-1 β (n = 3). **E–H** Western blot analysis of ER stress-related proteins, matrix metabolism-related proteins and apoptosis-related proteins in NP cells treated with knockdown and overexpression of PPAR γ respectively (n = 3). **I, J** Representative immunofluorescence images of COL2 and cleaved caspase3 in NP cells of each indicated groups (n = 3). **K, L** Apoptosis of NP cells by flow cytometry after knockdown and overexpression of PPAR γ respectively (n = 3). **M, N** Western blot analysis of LRP1, PPAR γ and ER stress markers in NP cells co-treated with knockdown of LRP1 and overexpression of PPAR (n = 4). *p < 0.05, **p < 0.01, ***p < 0.001. Data are presented as the mean \pm SD.

caspase-3 were upregulated in the AFP group but downregulated in the SP16 group (Fig. 7I–K, O–Q). Additionally, the expression of COL2 was higher in the SP16 group compared to the AFP group (Fig. 7L, R). These results indicate that activation of LRP1 inhibited ER stress, apoptosis, and ECM degradation, thereby delaying the progression of IDD in vivo.

4. Discussion

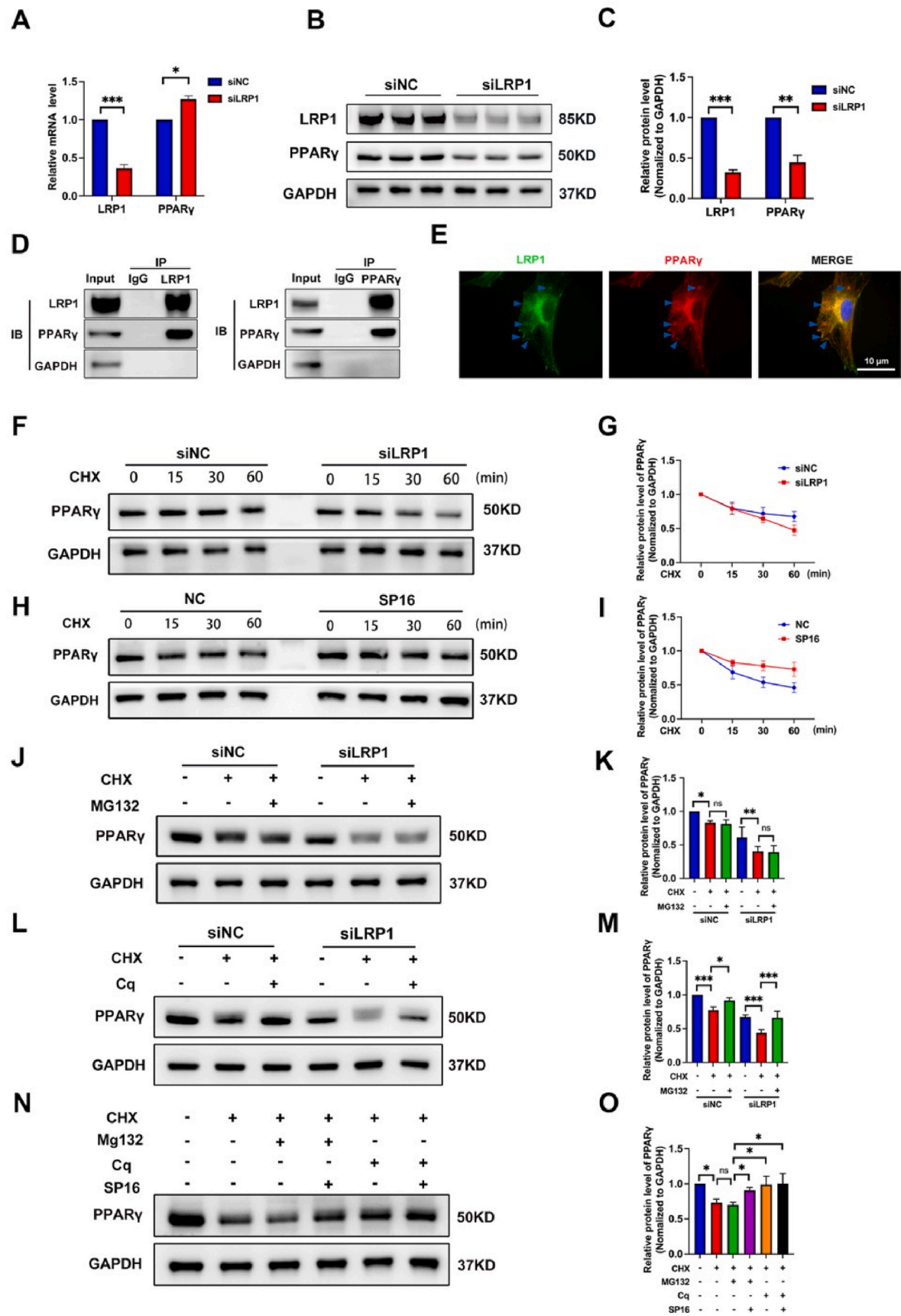
Conservative treatments for IDD face limitations in addressing underlying biological issues, while surgical interventions carry the risk of complications. Therefore, it is crucial to explore the molecular mechanisms of IDD and develop early interventions. Previous studies have highlighted the role of inflammation-induced ECM degradation and apoptosis in IDD progression [38,39]. However, the precise molecular mechanisms and potential therapeutic targets for IDD remain elusive. LRP1 has been reported to inhibit inflammation in various diseases [40–44], suggesting its significant potential in intervertebral disc research. In this study, we investigated the biological role of LRP1 in IDD. Our findings revealed decreased LRP1 expression in degenerative human NP tissue, rat IDD models, and in vitro inflammation models. This reduction was correlated with matrix degradation and apoptosis of nucleus pulposus (NP) cells, potentially contributing to IDD progression. Conversely, activating LRP1 alleviated apoptosis and matrix degradation, thereby inhibiting IDD. Furthermore, we highlighted the involvement of ER stress in this process. Our study sheds light on the role of LRP1 in IDD and underscores its potential as a therapeutic target. By understanding the molecular mechanisms underlying IDD, we can pave the way for the development of novel interventions.

LRP1 belongs to the family of low-density lipoprotein receptors, comprising subunits of 515 kDa and 85 kDa. This receptor plays a crucial role in diverse cellular processes such as intracellular signal transduction, lipid homeostasis, and clearance of apoptotic cells [40]. LRP1 promotes anti-inflammatory and anti-apoptotic states in cells under various injury conditions [45,46]. For example, activation of LRP1 promotes the polarization of M2 macrophages to reduce white matter injury through the phosphatidylinositol 3-kinase (PI3K)/Akt pathway in a rat model [47]. Additionally, RG108 upregulates LRP1 protein levels to attenuate cell apoptosis induced by cisplatin-induced oxidative stress through the PI3K/Akt pathway in mice [17]. In osteoarthritis, LRP1 inhibits cell apoptosis induced by tumor necrosis factor- α (TNF- α) [16]. The PI3K/Akt pathway has anti-apoptotic activity [48,49], supporting the anti-apoptotic effect of LRP1 in IDD. Therefore, we speculated that LRP1 negatively regulates apoptosis of NP cells. In our study, LRP1 knockdown promoted apoptosis of NP cells, consistent with previous studies. In IDD, NP tissue is highly susceptible to remodeling, characterized by decreased synthesis and increased degradation of the ECM [50]. In chondrocytes, LRP1 engulfs and clears extracellular ADAMTs-5 and MMP13, reducing ECM degradation and protecting against arthritis [51]. This suggests that LRP1 can mitigate ECM degradation. Another study demonstrated that COL2 synthesis was blocked in LRP1 knockout chondrocytes [23]. Consistent with these findings, our study verified that LRP1 knockdown decreased COL2 levels and increased MMP13 expression in NP cells, suggesting that LRP1 plays a significant role in maintaining matrix metabolism homeostasis in NP cells.

To elucidate the mechanism of apoptosis and ECM degradation in NP cells, we investigated ER stress in these cells. The main pathways of apoptosis include the mitochondrial pathway [52], the ER pathway [53]

and the death receptor pathway [54]. The unfolded protein response (UPR) induced by ER stress can activate all three pathways [55,56]. ER stress has been significantly upregulated in IDD [24]. Studies have shown that ER stress activates the three UPR signaling pathways (PERK, IRE1 α , and AT6), promoting the expression of XBP-1 and CHOP, leading to ECM degradation and apoptosis in IDD [26,57]. A study has shown the functional deletion of LRP1 upregulates CHOP and cleaved caspase3 in hepatocytes, indicating that LRP1 has the function of regulating ER stress [27]. Consistent with this, our study found that knockdown of LRP1 exacerbates IL-1 β -induced ER stress. However, the role of ER stress in regulating ECM metabolism and apoptosis through LRP1 remains to be fully elucidated. Treatment with the ER stress inhibitor 4-PBA reduces cell apoptosis and ECM degradation induced by LRP1 knockdown. These findings suggest that LRP1 regulates apoptosis of NP cells by modulating ER stress.

To determine why LRP1 inhibits ER stress in NP cells, we selected PPAR γ as the predicted downstream target of LRP1, as it has been reported to inhibit ER stress in L-NAME-induced hypertensive rats [32]. Additionally, the PPAR γ activator pioglitazone can inhibit the NF- κ B pathway, thereby reducing IL-17-induced matrix degradation in IDD [29]. Furthermore, in cartilage-specific PPAR γ knockout mice, ECM degradation and apoptosis were enhanced [58]. Our study showed that PPAR γ was downregulated and positively correlated with LRP1 in IDD. Thus, we speculated that LRP1 regulates apoptosis and ECM degradation via ER stress by targeting PPAR γ . Consistent with this hypothesis, knockdown of PPAR γ activated ER stress, promoted apoptosis, and increased ECM degradation, which were reversed by the overexpression of PPAR γ . Further studies demonstrated that ER stress caused by LRP1 knockdown was mitigated by the overexpression of PPAR γ . These findings support the notion that LRP1 reduces apoptosis and ECM degradation by inhibiting ER stress through PPAR γ . Additionally, previous studies have shown that LRP1 interacts with PPAR γ in endothelial cells [31]. In this study, we elucidated the interaction between LRP1 and PPAR γ in NP cells. Notably, our immunofluorescence results revealed that LRP1 and PPAR γ are localized in the cytoplasm and interact with each other, contrasting with previous studies that demonstrated LRP1 binding with PPAR γ in the nucleus [31]. A study has shown that PPAR γ interacts with P65 in the cytoplasm of NP cells and inhibits the nuclear translocation of P65, confirming the cytoplasmic distribution of PPAR γ in NP cells, which is consistent with our findings and further supports the interaction between LRP1 and PPAR γ within the cytoplasm [59]. Studies have shown that in NP cells treated with inflammatory factors such as IL-1 β and TNF- α , both mRNA and protein levels of PPAR γ are downregulated [29,60], which is consistent with our finding that IL-1 β reduces PPAR γ protein levels. However, in our study, following LRP1 knockdown, the mRNA levels of PPAR γ increased while the protein levels decreased, suggesting that LRP1 regulates PPAR γ at the post-transcriptional level. Next, we confirmed that LRP1 can stabilize the protein levels of PPAR γ , preventing its degradation via the lysosomal pathway. There are two pathways for protein degradation: the proteasomal pathway and the lysosomal pathway. We used MG132 to block degradation via the proteasomal pathway and Cq to inhibit protein degradation through the lysosomal pathway. Our study found that after LRP1 knockdown, PPAR γ is degraded through the lysosomal pathway rather than the proteasomal pathway. Since E3 ligases typically target proteins for degradation via the proteasome, their involvement in PPAR γ degradation appears to be minimal. Moreover, LRP1 is known to activate the PI3K/AKT signaling pathway [17], which in turn activates



(caption on next page)

Fig. 6. LRP1 interacted with PPAR γ to inhibit PPAR γ degradation via lysosomal pathway. **A** Relative mRNA expression of PPAR γ in the rat NP cells with knockdown of LRP1, as measured by qRT-PCR (n = 5). **B, C** Western blot analysis of LRP1 and PPAR γ in siLRP1-treated NP cells (n = 6). **D** Immunoprecipitation to detect interaction of LRP1 and PPAR γ (n = 3). **E** Representative immunofluorescence images of co-incubation with LRP1 and PPAR γ in NP cells (n = 6). **F, G** Western blot analysis of PPAR γ in siNC and siLRP1 groups under stimulation of CHX (50 μ g/ml) (n = 6). **H, I** Western blot analysis of PPAR γ in NC and SP16 groups under stimulation of CHX (n = 6). **J, K** Western blot analysis of PPAR γ in siNC- and siLRP1-treated NP cells with stimulation of CHX and MG132 (n = 6). **L, M** Western blot analysis of PPAR γ in siNC- and siLRP1-treated NP cells with stimulation of CHX and Cq (20 μ M) (n = 6). **N, O** Western blot analysis of PPAR γ in NP cells of each indicated groups (n = 6). *p < 0.05, **p < 0.01, ***p < 0.001. Data are presented as the mean \pm SD.

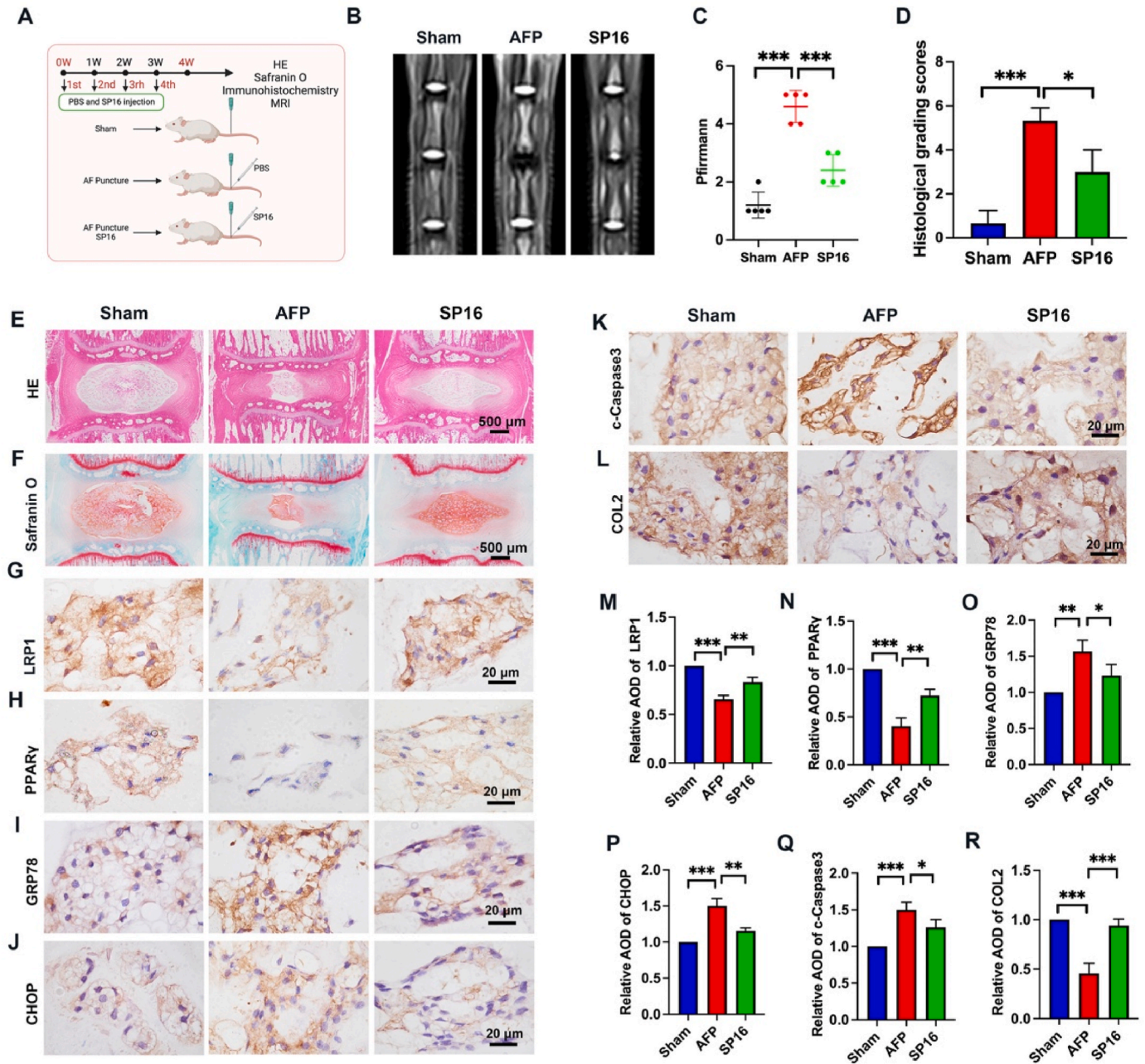


Fig. 7. LRP1 activator SP16 attenuates IDD in rat model. **A** Schematic diagram of animal experiment process. **B** Representative MRI images of different groups (sham, AFP, AFP + SP16) 4 weeks after surgery (n = 6). **C**, The Pfirrmann grading of intervertebral discs in each group (n = 5). **D** Histological scores in rat intervertebral disc of each indicated groups (n = 3). **E, F** HE, safranin O staining in rat intervertebral disc of each indicated groups (n = 3). **G-R** Representative immunohistochemical images and statistical analysis of LRP1, PPAR γ , GRP78, CHOP, COL2 and cleaved caspase3 in rat intervertebral discs of each indicated groups (n = 3). *p < 0.05, **p < 0.01, ***p < 0.001. Data are presented as the mean \pm SD.

mTOR [61], thereby inhibiting autophagy. Thus, when LRP1 is knocked down or inhibited, it may suppress mTOR activity, leading to enhanced autophagy and potentially promoting the lysosomal degradation of PPAR γ . However, further validation in this area has not been conducted.

Based on these findings, we propose that inflammation-induced decreases in LRP1 protein content led to reduced binding of PPAR γ to LRP1. The unbound PPAR γ is then more susceptible to degradation, resulting in heightened sensitivity to ER stress, a phenomenon not

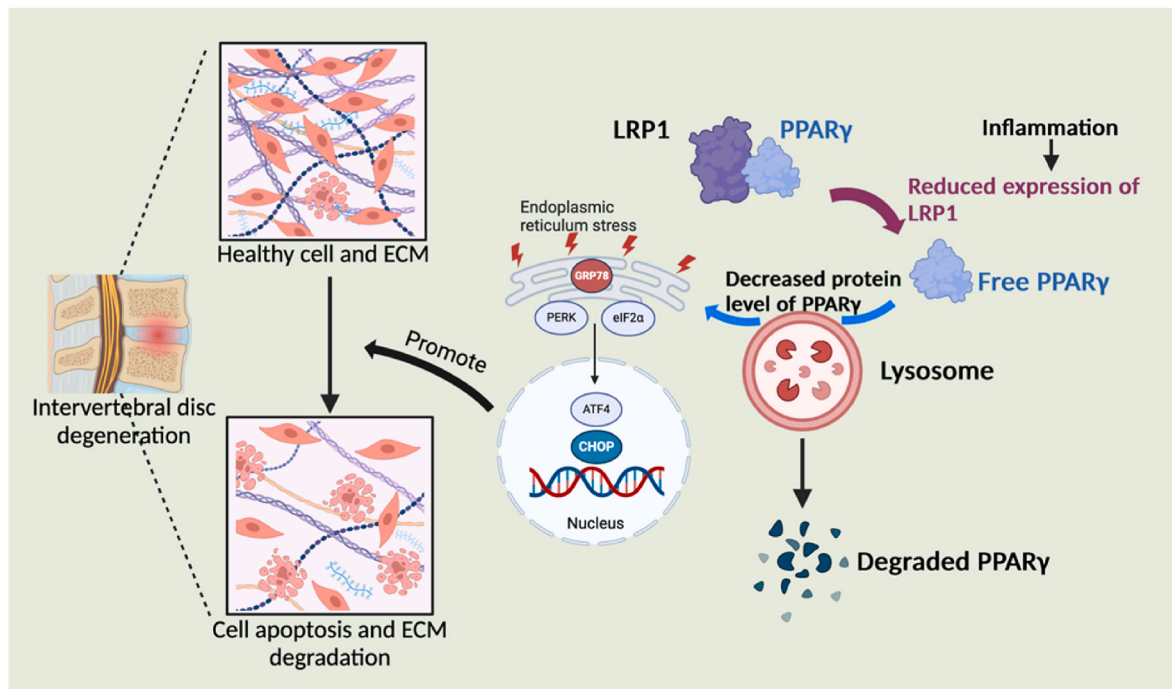


Fig. 8. Schematic illustration of the possible mechanism of LRP1 in IDD. The downregulation of LRP1 expression in IDD under inflammation leads to increased degradation of PPAR γ , due to the reduced ability of LRP1 to bind with PPAR γ . This, in turn, triggers endoplasmic reticulum stress, resulting in enhanced apoptosis of nucleus pulposus cells and degradation of the extracellular matrix. Consequently, this exacerbates the progression of IDD.

reported in existing studies. However, our research has several limitations. While we investigated the downstream mechanisms of LRP1, including its effects on PPAR γ and ER stress, we did not explore the upstream mechanisms regulating LRP1 itself. This will be the focus of future research. Additionally, although we have clarified the specific mechanism by which LRP1 regulates PPAR γ protein levels, the precise manner in which PPAR γ influences ER stress remains unclear and warrants further investigation.

5. Conclusion

In summary, our research findings suggest that LRP1 inhibits IDD by stabilizing PPAR γ protein, thereby suppressing inflammation-induced ER stress. This stabilization prevents the degradation of the ECM and reduces apoptosis in NP cells (Fig. 8). These results provide evidence that LRP1 could be a potential therapeutic target for the treatment of IDD.

CRedit authorship contribution statement

Dengbo Yao: Data curation, and, Writing – original draft. **Ming Li:** and, **Weike Zeng:** and, **Kun Wang:** Conceptualization, and, Methodology. **Zhuangyao Liao:** Software, and, Validation. **Enming Chen:** Supervision. **Tong Xing:** and, **Yuwei Liang:** and, **Jun Tang:** Investigation. **Guoming Wen:** and, **Qing Ning:** Visualization. **Yuxi Li:** Writing – review & editing. **Lin Huang:** Writing – review & editing, and, Funding acquisition.

Data availability statement

All data generated or analyzed during the current study are included in this published article.

Declaration of competing interest

The authors have declared that no competing interest exists.

Acknowledgments

The rat NP cells used in this experiment were partly provided by Professor Qin An from the Department of Orthopedic Surgery, Shanghai Ninth People's Hospital, Shanghai Jiao Tong University School of Medicine. We are very grateful to him. We are very grateful for the drawing platform provided by the BioRender website. Funding: This study was supported by grants from Natural Science Foundation of Guangdong Province (2022A1515012305 and 2021A1515111013), Guangzhou Science and Technology Project (202201020480 and 202201010881).

Abbreviations

IDD	Intervertebral disc degeneration
NP	Nucleus pulposus
ECM	Extracellular matrix
AFP	Annulus fibrosus puncture
LRP1	Low-density lipoprotein receptor-related protein 1
PPAR γ	Peroxisome proliferator-activated receptor gamma
ER	Endoplasmic reticulum
NC	Negative control
IL-1 β	Interleukin 1beta
MMP13	Matrix metalloproteinase-13
COL2	Collagen type 2
Bcl-2	B cell lymphoma 2
PI3K/AKT	Phosphatidylinositol 3-kinase/protein kinase B
TEM	Transmission electron microscopy
UPR	Unfolded protein response
p-PERK	Phosphorylated protein kinase-like endoplasmic reticulum kinase
p-eIF2 α	Phosphorylated eukaryotic initiation factor 2 alpha
ATF4	Activating transcription factor 4
CHX	Cycloheximide
Cq	Chloroquine
MRI	Magnetic resonance imaging

4-PBA 4-Phenylbutyric acid

References

- [1] Andersson GB. Epidemiological features of chronic low-back pain. *Lancet* 1999;354(9178):581–5 [eng].
- [2] Hartvigsen J, Hancock MJ, Kongsted A, Louw Q, Ferreira ML, Genevay S, et al. What low back pain is and why we need to pay attention. *Lancet* 2018;391(10137):2356–67 [eng].
- [3] Knezevic NN, Candido KD, Vlaeyen JWS, Van Zundert J, Cohen SP. Low back pain. *Lancet* 2021;398(10294):78–92 [eng].
- [4] Livshits G, Popham M, Malkin I, Sambrook PN, Macgregor AJ, Spector T, et al. Lumbar disc degeneration and genetic factors are the main risk factors for low back pain in women: the UK Twin Spine Study. *Ann Rheum Dis* 2011;70(10):1740–5 [eng].
- [5] Risbud MV, Shapiro IM. Role of cytokines in intervertebral disc degeneration: pain and disc content. *Nat Rev Rheumatol* 2014;10(1):44–56 [eng].
- [6] Chen S, Lei L, Li Z, Chen F, Huang Y, Jiang G, et al. Grem1 accelerates nucleus pulposus cell apoptosis and intervertebral disc degeneration by inhibiting TGF- β -mediated Smad2/3 phosphorylation. *Exp Mol Med* 2022;54(4):518–30 [eng].
- [7] Chou D, Samartzis D, Bellabarba C, Patel A, Luk KD, Kisser JM, et al. Degenerative magnetic resonance imaging changes in patients with chronic low back pain: a systematic review. *Spine* 2011;36(21 Suppl):S43–53 [eng].
- [8] Wu X, Miao X, Guo Y, Shao T, Tang S, Lin Y, et al. Slug enables redox-sensitive trans-activation of LRP1 by COUP-TFII: implication in antifibrotic intervention in the kidneys. *Life Sci* 2023;316:121412 [eng].
- [9] Wygrecka M, Wilhelm J, Jablonska E, Zakrzewicz D, Preissner KT, Seeger W, et al. Shedding of low-density lipoprotein receptor-related protein-1 in acute respiratory distress syndrome. *Am J Respir Crit Care Med* 2011;184(4):438–48 [eng].
- [10] Shinohara M, Tachibana M, Kanekiyo T, Bu G. Role of LRP1 in the pathogenesis of Alzheimer's disease: evidence from clinical and preclinical studies. *J Lipid Res* 2017;58(7):1267–81 [eng].
- [11] Mineo C. Lipoprotein receptor signalling in atherosclerosis. *Cardiovasc Res* 2020;116(7):1254–74 [eng].
- [12] Yamamoto K, Santamaria S, Botkjaer KA, Dudhia J, Troeberg L, Itoh Y, et al. Inhibition of shedding of low-density lipoprotein receptor-related protein 1 reverses cartilage matrix degradation in osteoarthritis. *Arthritis Rheumatol* 2017;69(6):1246–56 [eng].
- [13] Yamamoto K, Owen K, Parker AE, Scilabra SD, Dudhia J, Strickland DK, et al. Low density lipoprotein receptor-related protein 1 (LRP1)-mediated endocytic clearance of a disintegrin and metalloproteinase with thrombospondin motifs-4 (ADAMTS-4): functional differences of non-catalytic domains of ADAMTS-4 and ADAMTS-5 in LRP1 binding. *J Biol Chem* 2014;289(10):6462–74 [eng].
- [14] Scilabra SD, Troeberg L, Yamamoto K, Emonard H, Thøgersen I, Enghild JJ, et al. Differential regulation of extracellular tissue inhibitor of metalloproteinases-3 levels by cell membrane-bound and shed low density lipoprotein receptor-related protein 1. *J Biol Chem* 2013;288(1):332–42 [eng].
- [15] Yamamoto K, Scavenius C, Meschis MM, Gremida AME, Mogensen EH, Thøgersen IB, et al. A top-down approach to uncover the hidden ligandome of low-density lipoprotein receptor-related protein 1 in cartilage. *Matrix Biol* 2022;112:190–218 [eng].
- [16] Yang E, Zheng H, Peng H, Ding Y. Lentivirus-induced knockdown of LRP1 induces osteoarthritic-like effects and increases susceptibility to apoptosis in chondrocytes via the nuclear factor- κ B pathway. *Exp Ther Med* 2015;10(1):97–105 [eng].
- [17] He Y, Zheng Z, Liu C, Li W, Zhao L, Nie G, et al. Inhibiting DNA methylation alleviates cisplatin-induced hearing loss by decreasing oxidative stress-induced mitochondria-dependent apoptosis via the LRP1-PI3K/AKT pathway. *Acta Pharm Sin B* 2022;12(3):1305–21 [eng].
- [18] Muratoglu SC, Mikhailenko I, Newton C, Migliorini M, Strickland DK. Low density lipoprotein receptor-related protein 1 (LRP1) forms a signaling complex with platelet-derived growth factor receptor-beta in endosomes and regulates activation of the MAPK pathway. *J Biol Chem* 2010;285(19):14308–17 [eng].
- [19] Ju Y, Gu L, Hu M, Zheng M, Zhou X, Li Q, et al. Andrographolide exerts a neuroprotective effect by regulating the LRP1-mediated PPAR γ /NF- κ B pathway. *Eur J Pharmacol* 2023;951:175756 [eng].
- [20] Terrand J, Bruban V, Zhou L, Gong W, El Asmar Z, May P, et al. LRP1 controls intracellular cholesterol storage and fatty acid synthesis through modulation of Wnt signaling. *J Biol Chem* 2009;284(1):381–8 [eng].
- [21] Bian W, Tang M, Jiang H, Xu W, Hao W, Sui Y, et al. Low-density-lipoprotein-receptor-related protein 1 mediates Notch pathway activation. *Dev Cell* 2021;56(20):2902. 19.e8. [eng].
- [22] Yamamoto K, Troeberg L, Scilabra SD, Pelosi M, Murphy CL, Strickland DK, et al. LRP-1-mediated endocytosis regulates extracellular activity of ADAMTS-5 in articular cartilage. *Faseb j* 2013;27(2):511–21 [eng].
- [23] Yan W, Zheng L, Xu X, Hao Z, Zhang Y, Lu J, et al. Heterozygous LRP1 deficiency causes developmental dysplasia of the hip by impairing triad chondrocytes differentiation due to inhibition of autophagy. *Proc Natl Acad Sci U S A* 2022;119(37):e2203557119 [eng].
- [24] Liao Z, Luo R, Li G, Song Y, Zhan S, Zhao K, et al. Exosomes from mesenchymal stem cells modulate endoplasmic reticulum stress to protect against nucleus pulposus cell death and ameliorate intervertebral disc degeneration in vivo. *Theranostics* 2019;9(14):4084–100 [eng].
- [25] Wen T, Xue P, Ying J, Cheng S, Liu Y, Ruan D. The role of unfolded protein response in human intervertebral disc degeneration: perk and IRE1- α as two potential therapeutic targets. *Oxid Med Cell Longev* 2021;2021:6492879 [eng].
- [26] Chen Y, Li B, Xu Y, Zhou T, Zhao C, Zhao J. Sal003 alleviated intervertebral disc degeneration by inhibiting apoptosis and extracellular matrix degradation through suppressing endoplasmic reticulum stress pathway in rats. *Front Pharmacol* 2023;14:1095307 [eng].
- [27] Hamlin AN, Basford JE, Jaeschke A, Hui DY. LRP1 protein deficiency exacerbates palmitate-induced steatosis and toxicity in hepatocytes. *J Biol Chem* 2016;291(32):16610–9 [eng].
- [28] Wang S, Dougherty EJ, Danner RL. PPAR γ signaling and emerging opportunities for improved therapeutics. *Pharmacol Res* 2016;111:76–85 [eng].
- [29] Liu Y, Qu Y, Liu L, Zhao H, Ma H, Si M, et al. PPAR- γ agonist pioglitazone protects against IL-17 induced intervertebral disc inflammation and degeneration via suppression of NF- κ B signaling pathway. *Int Immunopharmacol* 2019;72:138–47 [eng].
- [30] Li X, Hou Q, Yuan W, Zhan X, Yuan H. Inhibition of miR-96-5p alleviates intervertebral disc degeneration by regulating the peroxisome proliferator-activated receptor γ /nuclear factor-kappaB pathway. *J Orthop Surg Res* 2023;18(1):916 [eng].
- [31] Mao H, Lockyer P, Li L, Ballantyne CM, Patterson C, Xie L, et al. Endothelial LRP1 regulates metabolic responses by acting as a co-activator of PPAR γ . *Nat Commun* 2017;8:14960 [eng].
- [32] Soliman E, Behairy SF, El-Maraghy NN, Elshazly SM. PPAR- γ agonist, pioglitazone, reduced oxidative and endoplasmic reticulum stress associated with L-NAME-induced hypertension in rats. *Life Sci* 2019;239:117047 [eng].
- [33] Pfirrmann CW, Metzendorf A, Zanetti M, Hodler J, Boos N. Magnetic resonance classification of lumbar intervertebral disc degeneration. *Spine* 2001;26(17):1873–8 [eng].
- [34] Keorochana G, Johnson JS, Taghavi CE, Liao JC, Lee KB, Yoo JH, et al. The effect of needle size inducing degeneration in the rat caudal disc: evaluation using radiograph, magnetic resonance imaging, histology, and immunohistochemistry. *Spine J* 2010;10(11):1014–23 [eng].
- [35] Wang Z, Martellucci S, Van Enoo A, Austin D, Gelber C, Campana WM. α 1-Antitrypsin derived SP16 peptide demonstrates efficacy in rodent models of acute and neuropathic pain. *Faseb j* 2022;36(1):e22093 [eng].
- [36] Toldo S, Austin D, Mauro AG, Mezzaroma E, Van Tassell BW, Marchetti C, et al. Low-density lipoprotein receptor-related protein-1 is a therapeutic target in acute myocardial infarction. *JACC Basic Transl Sci* 2017;2(5):561–74 [eng].
- [37] Soler Y, Rodriguez M, Austin D, Gineste C, Gelber C, El-Hage N. SERPIN-derived small peptide (SP16) as a potential therapeutic agent against HIV-induced inflammatory molecules and viral replication in cells of the central nervous system. *Cells* 2023;12(4) [eng].
- [38] Sampara P, Banala RR, Vemuri SK, Av GR, Gpv S. Understanding the molecular biology of intervertebral disc degeneration and potential gene therapy strategies for regeneration: a review. *Gene Ther* 2018;25(2):67–82 [eng].
- [39] Kang L, Zhang H, Jia C, Zhang R, Shen C. Targeting oxidative stress and inflammation in intervertebral disc degeneration: therapeutic perspectives of phytochemicals. *Front Pharmacol* 2022;13:956355 [eng].
- [40] Wujak L, Schnieder J, Schaefer L, Wygrecka M. LRP1: a chameleon receptor of lung inflammation and repair. *Matrix Biol* 2018;68-69:366–81 [eng].
- [41] Actis Dato V, Chiabrando GA. The role of low-density lipoprotein receptor-related protein 1 in lipid metabolism, glucose homeostasis and inflammation. *Int J Mol Sci* 2018;19(6) [eng].
- [42] Jaeschke A, Haller A, Cash JG, Nam C, Igel E, Roebroek AJM, et al. Mutation in the distal NPXY motif of LRP1 alleviates dietary cholesterol-induced dyslipidemia and tissue inflammation. *J Lipid Res* 2021;62:100012 [eng].
- [43] Konanias ES, Kuhel DG, Basford JE, Weintraub NL, Hui DY. Deficiency of LRP1 in mature adipocytes promotes diet-induced inflammation and atherosclerosis-brief report. *Arterioscler Thromb Vasc Biol* 2017;37(6):1046–9 [eng].
- [44] Lockyer P, Mao H, Fan Q, Li L, Yu-Lee LY, Eissa NT, et al. LRP1-Dependent BMPER signaling regulates lipopolysaccharide-induced vascular inflammation. *Arterioscler Thromb Vasc Biol* 2017;37(8):1524–35 [eng].
- [45] Campana WM, Li X, Dragojlovic N, Jones J, Gaultier A, Gonias SL. The low-density lipoprotein receptor-related protein is a pro-survival receptor in Schwann cells: possible implications in peripheral nerve injury. *J Neurosci* 2006;26(43):11197–207 [eng].
- [46] Zurhove K, Nakajima C, Herz J, Bock HH, May P. Gamma-secretase limits the inflammatory response through the processing of LRP1. *Sci Signal* 2008;1(47):ra15 [eng].
- [47] Peng J, Pang J, Huang L, Enkhjargal B, Zhang T, Mo J, et al. LRP1 activation attenuates white matter injury by modulating microglial polarization through Shc1/PI3K/Akt pathway after subarachnoid hemorrhage in rats. *Redox Biol* 2019;21:101121 [eng].
- [48] Chen HW, Liu MQ, Zhang GZ, Zhang CY, Wang ZH, Lin AX, et al. Proanthocyanidins inhibit the apoptosis and aging of nucleus pulposus cells through the PI3K/Akt pathway delaying intervertebral disc degeneration. *Connect Tissue Res* 2022;63(6):650–62 [eng].
- [49] Yu B, Shen B, Ba Z, Liu Z, Yuan J, Zhao W, et al. USP15 promotes the apoptosis of degenerative nucleus pulposus cells by suppressing the PI3K/AKT signalling pathway. *J Cell Mol Med* 2020;24(23):13813–23 [eng].
- [50] Le Maitre CL, Pockert A, Buttle DJ, Freemont AJ, Hoyland JA. Matrix synthesis and degradation in human intervertebral disc degeneration. *Biochem Soc Trans* 2007;35(Pt 4):652–5 [eng].
- [51] Yamamoto K, Okano H, Miyagawa W, Visse R, Shitomi Y, Santamaria S, et al. MMP-13 is constitutively produced in human chondrocytes and co-endocytosed with ADAMTS-5 and TIMP-3 by the endocytic receptor LRP1. *Matrix Biol* 2016;56:57–73 [eng].

- [52] Green DR. The mitochondrial pathway of apoptosis Part II: the BCL-2 protein family. *Cold Spring Harb Perspect Biol* 2022;14(6) [eng].
- [53] Rellmann Y, Eidhof E, Dreier R. Review: ER stress-induced cell death in osteoarthritic cartilage. *Cell Signal* 2021;78:109880 [eng].
- [54] McIlwain DR, Berger T, Mak TW. Caspase functions in cell death and disease. *Cold Spring Harb Perspect Biol* 2013;5(4):a008656 [eng].
- [55] Lu M, Lawrence DA, Marsters S, Acosta-Alvear D, Kimmig P, Mendez AS, et al. Opposing unfolded-protein-response signals converge on death receptor 5 to control apoptosis. *Science* 2014;345(6192):98–101 [eng].
- [56] Galluzzi L, Vitale I, Aaronson SA, Abrams JM, Adam D, Agostinis P, et al. Molecular mechanisms of cell death: recommendations of the nomenclature committee on cell death 2018. *Cell Death Differ* 2018;25(3):486–541 [eng].
- [57] Fujii T, Fujita N, Suzuki S, Tsuji T, Takaki T, Umezawa K, et al. The unfolded protein response mediated by PERK is casually related to the pathogenesis of intervertebral disc degeneration. *J Orthop Res* 2018;36(5):1334–45 [eng].
- [58] Vasheghani F, Zhang Y, Li YH, Blati M, Fahmi H, Lussier B, et al. PPAR γ deficiency results in severe, accelerated osteoarthritis associated with aberrant mTOR signalling in the articular cartilage. *Ann Rheum Dis* 2015;74(3):569–78 [eng].
- [59] Xu T, Zhao H, Fang X, Wang S, Li J, Wu H, et al. Mulberroside A mitigates intervertebral disc degeneration by inhibiting MAPK and modulating Ppar- γ /NF- κ B pathways. *J Inflamm* 2024;21(1):32 [eng].
- [60] Cheng P, Wei HZ, Chen HW, Wang ZQ, Mao P, Zhang HH. DNMT3a-mediated methylation of PPAR γ promote intervertebral disc degeneration by regulating the NF- κ B pathway. *J Cell Mol Med* 2024;28(2):e18048 [eng].
- [61] Geng H, Zhang H, Cheng L, Dong S. Corrigendum to "Sivelestat ameliorates sepsis-induced myocardial dysfunction by activating the PI3K/AKT/mTOR signaling pathway". *Int. Immunopharmacol.* 2024;128. <https://doi.org/10.1016/j.intimp.2023.111466>. *Int Immunopharmacol* 2024;131:111873. [eng].